Voltammetric Sensing of Thiols. The Electrocatalytic Oxidation of 4-Acetamidophenol in the Presence of Cysteine: a Mechanistic Rotating Disk Electrode Study

Benjamin A. Brookes, Paul C. White, Nathan S. Lawrence, and Richard G. Compton*

Physical and Theoretical Chemistry Laboratory, Oxford University, South Parks Road, Oxford, OX1 3QZ, United Kingdom

Received: March 8, 2001; In Final Form: May 1, 2001

A numerical method is illustrated for the modeling of an important electrocatalytic reaction at the rotating disk electrode (RDE). This reaction, labeled $EC_{2X}E$, occurs via the following route: $A - 2e^- \rightleftharpoons B$, $B + X \rightarrow B{-}X$ (k_2), $B{-}X - 2e^- \rightleftharpoons [B{-}X]^{2+}$. The numerical method is based on a finite difference formulation of coupled mass transport and kinetic equations and makes use of a Hale coordinate transformation. Iterative solutions are performed using a Gauss−Newton scheme to solve the nonlinear differential equations. Numerical solutions are calculated to generate working surfaces in the effective number of electrons transferred, N_{eff}. Cyclic voltammetry is reported in hydrostatic conditions with a 4-acetamidophenol (paracetamol)/cysteine system, which is shown to proceed via the $EC_{2X}E$ reaction pathway. The resulting data is modeled using the commercial package DIGISIM, and a result of $k_2 = 1.25 \pm 0.25 \times 10^7$ mol^{-1} cm^3 s^{-1} is obtained. RDE studies of the same system using steady-state linear sweep hydrodynamic voltammetry is next performed to collect limiting current data at rotation speeds of 2, 4, 8, 16, and 25 Hz. Working surface interpolation of the resulting data results in a mean value of $1.6 \pm 0.35 \times 10^7$ mol^{-1} cm^3 s^{-1} for the rate constant k_2.

Introduction

We have recently reviewed the available analytical stategies for the detection of hydrogen sulfide and related species and concluded that voltammetric approaches can offer significant advantages.[1] Of the possible electrochemical strategies that can be adapted, an increasingly widely applied method requires the measurement of the electrocatalytic current arising from reaction paths such as

$$A - 2e^- \rightleftharpoons B$$

$$B + X \rightarrow B{-}X\ (k_2)$$

$$B{-}X - 2e^- \rightleftharpoons [B{-}X]^{2+}$$

where X is the target molecule that is trapped via the electrochemical activation of A forming B−X which is determined amperometrically. This strategy has found wide use in the case where X is H_2S or RSH.[2−5]

The reaction mechanism given above has been labeled $EC_{2X}E$ to emphasize the similarity to, and differences from, the classical ECE reaction. In particular, the chemical step is a second-order reaction, and the quantity of X present is typically comparable to the levels of B. The characterization of the $EC_{2X}E$ mechanism is possible using a microdisk approach.[6] However, this requires a relatively fast chemical reaction step to offer the necessary precision. For slower reaction processes, it is preferable to employ macroelectrode voltammetry so that the current enhancement is amplified. In particular, a rotating disk electrode offers a very convenient approach to such measurements. Accordingly in this paper, we evolve the theory of the $EC_{2X}E$ processes at RDEs and, using this numerical approach, generate working surfaces suitable for data analysis. This is then applied to experimental data gathered for the paracetamol (4-acetamidophenol)/cysteine system in aqueous solution.

Theory

The time-dependent convection−diffusion equation describing the mass transport of species A to a rotating disk electrode in the absence of migration is given by

$$\frac{\partial a}{\partial t} = D_A \frac{\partial^2 a}{\partial z^2} + C_z z^2 \frac{\partial a}{\partial z} \tag{1}$$

where $a = [A]/[A]_{bulk}$, D_A is the diffusion coefficient of A, and z is the distance normal to the electrode. Equation 1 reveals that the electrode is uniformly accessible and the term $C_z z^2$ describes the convective flow close to the electrode surface. The constant C_z is given by

$$C_z = 8.032 W^{3/2} \upsilon^{-1/2} \tag{2}$$

where W is the disk rotation speed in Hz and υ is the kinematic viscosity of the medium (cm^2 s^{-1}). It can be shown[7] that eq 1 can be cast into nondimensional form by transforming z and t as

$$w = (C_z/D_A)^{1/3} z \tag{3}$$

and

$$\tau = (C_z^2 D_A)^{1/2} t \tag{4}$$

so that

$$\frac{\partial a}{\partial \tau} = \frac{\partial^2 a}{\partial w^2} + w^2 \frac{\partial a}{\partial w} \tag{5}$$

* To whom correspondence should be addressed.

10.1021/jp010883w CCC: $20.00
Published on Web 06/16/2001

Introducing the Hale transformation:[8,9]

$$y = g(w) = \frac{\int_0^w \exp\left(-\frac{1}{3}w^3\right)\mathrm{d}w}{\int_0^\infty \exp\left(-\frac{1}{3}w^3\right)\mathrm{d}w} \tag{6}$$

where $[\int_0^\infty \exp(-(1/3)w^3)]^2 = 1.65894$ transforms the mass transport equation to

$$\frac{\partial a}{\partial \tau} = \frac{\exp\left(-\frac{2}{3}w^3\right)}{\left[\int_0^\infty \exp\left(-\frac{1}{3}w^3\right)\mathrm{d}w\right]^2}\frac{\partial^2 a}{\partial y^2} = f(w)\nabla_y^2(a) \tag{7}$$

This change of variable results in the mass transport equation being transformed into a closed-space expression ($y = 1$ corresponds to a value of infinity for w), thus facilitating facile boundary condition implementation as z tends to infinity. We can now extend the mass transport theory for a single species to that for the $EC_{2X}E$ reaction. Here species B and X are removed in a homogeneous step with a rate constant k_2 to form species B−X, which we label as C, and assume to be totally consumed at the electrode surface. Assuming that $D_A = D_B = D_C \neq D_X$, the mass transport of the $EC_{2X}E$ reaction at steady state is described by a set of four mass transport partial differential equations:

$$\frac{\partial a}{\partial \tau} = f(w)\nabla_y^2(a) = 0 \tag{8a}$$

$$\frac{\partial b}{\partial \tau} = f(w)\nabla_Y^2(b) - k_{\mathrm{norm}}bx = 0 \tag{8b}$$

$$\frac{\partial x}{\partial \tau} = \kappa_X f(w)\nabla_Y^2(x) - k_{\mathrm{norm}}bx = 0 \tag{8c}$$

$$\frac{\partial c}{\partial \tau} = f(w)\nabla_Y^2(c) + k_{\mathrm{norm}}bx = 0 \tag{8d}$$

where $\kappa_X = D_X/D_A$ and $k_{\mathrm{norm}} = k_2[\mathrm{A}]_{\mathrm{bulk}}C_z^{-2/3}D_A^{-1/3}$. The boundary conditions applicable to eqs 8a−d are

$$\underline{\mathrm{y} = 0}: \quad \frac{\partial b}{\partial y} = -\frac{\partial a}{\partial y}; \frac{\partial x}{\partial y} = 0; c = 0$$

$$\underline{\mathrm{y} = 1}: \quad a = 1; b = 0; x = \gamma; c = 0$$

The variable γ is the normalized bulk concentration of the redox mediator species X:

$$\gamma = [\mathrm{X}]_{\mathrm{bulk}}/[\mathrm{A}]_{\mathrm{bulk}}$$

Because the solution to eq 8b with the given boundary conditions is, trivially, $a(y) = y$, it is not necessary to numerically solve the mass transport partial differential equation for the A species: the solution is, however, necessary only to evaluate the boundary condition for species B at the electrode surface. Because uniform accessibility to the rotating disk electrode is implicit in the formulation of eq 1, the current at the rotating disk electrode is given by

$$I = 2FD_A A[A]_{\mathrm{bulk}}\left(\left.\frac{\partial a}{\partial z}\right|_{z=0} + \left.\frac{\partial c}{\partial z}\right|_{z=0}\right) \tag{9}$$

where F is the Faraday constant and A is the electrode area. In the y coordinate system this is evaluated as

$$I = 2FA[A]_{\mathrm{bulk}}D_A^{2/3}C_z^{1/3}\left(\frac{\mathrm{d}y}{\mathrm{d}w}\right)_{y=0}\Psi \tag{10}$$

The total dimensionless electrode flux, ψ, is calculated as

$$\Psi = \sum_{S=A,C}\Psi_S = \frac{\partial a}{\partial y}|_{y=0} + \frac{\partial c}{\partial y}|_{y=0} \tag{11}$$

where Ψ_S is the dimensionless flux of a single species, S.

To derive a numerical formulation of eq 8, we seek a vector **u** that approximates the exact solutions $b(y)$, $c(y)$, and $x(y)$. The algebraic equations for the vector **u** are generated by discretizing the three relevant partial differential equations on a one-dimensional grid of N_J points using the central difference equation

$$\left(\frac{\partial^2 u^S}{\partial y^2}\right)_j = \frac{u_{j+1}^S - 2u_j^S + 2u_{j-1}^S}{(\Delta y)^2} \tag{12}$$

where u_j^S is the unknown concentration of single species S (= B, C, or X) and the location j such that

$$y = j\Delta y$$

and

$$j = 1, 2,...N_J - 1 \text{ and } \Delta y = (N_J)^{-1}$$

We also need to calculate the value of the function $f(w)$ as defined in eq 7 at each grid node j. This is most easily done by solving the respective ODE form of eq 7:

$$\frac{\partial w}{\partial y} = \exp\left(-\frac{1}{3}w^3\right)\left[\int_0^\infty \exp\left(-\frac{1}{3}w^3\right)\mathrm{d}w\right] \tag{13}$$

and substituting values of w. The implementation of the discretization upon partial differential eqs 8a−c results in $3(N_J - 1)$ nonlinear finite difference equations:

$$q_j^{\mathrm{B}} = \frac{\lambda_j}{(\Delta y)^2}(u_{j-1}^{\mathrm{B}} - 2u_j^{\mathrm{B}} + u_{j+1}^{\mathrm{B}}) - k_{\mathrm{norm}}u_j^{\mathrm{B}}u_j^{\mathrm{X}} \tag{14a}$$

$$q_j^{\mathrm{X}} = \kappa_{\mathrm{X}}\frac{\lambda_j}{(\Delta y)^2}(u_{j-1}^{\mathrm{X}} - 2u_j^{\mathrm{X}} + u_{j+1}^{\mathrm{X}}) - k_{\mathrm{norm}}u_j^{\mathrm{B}}u_j^{\mathrm{X}} = 0 \tag{14b}$$

$$q_j^{\mathrm{C}} = \frac{\lambda_j}{(\Delta y)^2}(u_{j-1}^{\mathrm{C}} - 2u_j^{\mathrm{C}} + u_{j+1}^{\mathrm{C}}) + k_{\mathrm{norm}}u_j^{\mathrm{B}}u_j^{\mathrm{X}} = 0 \tag{14c}$$

where $1 \leq j < N_J$, $\lambda_j = f(g^{-1}(j\Delta y))$ and the finite difference formulations of the boundary conditions applicable are

$$\underline{\mathrm{j} = 0}: u_0^{\mathrm{B}} + \Delta y = u_1^{\mathrm{B}}; u_0^{\mathrm{X}} = u_1^{\mathrm{X}}; u_0^{\mathrm{C}} = 0$$

$$\underline{\mathrm{j} = N_J}: u_{N_J}^{\mathrm{B}} = 0; u_{N_J}^{\mathrm{X}} = \gamma; u_{N_J}^{\mathrm{C}} = 0$$

The finite difference eqs 14 may alternatively be written in the matrix vector form as

$$\mathbf{q} = \mathbf{M}\mathbf{u} + \hat{\mathrm{N}}(\mathbf{u}) \tag{15}$$

where **M** is a sparse banded matrix composed of the coefficients of the linear terms in **u, q** is the known vector, and $\hat{\mathrm{N}}$ is the nonlinear kinetic operator for the terms such that

$$\hat{\mathrm{N}}(\mathbf{u}_j) = \hat{\mathrm{N}}\begin{bmatrix} u_j^{\mathrm{B}} \\ u_j^{\mathrm{X}} \\ u_j^{\mathrm{C}} \end{bmatrix} = \begin{bmatrix} -k_{\mathrm{norm}} u_j^{\mathrm{B}} u_j^{\mathrm{X}} \\ -k_{\mathrm{norm}} u_j^{\mathrm{B}} u_j^{\mathrm{X}} \\ k_{\mathrm{norm}} u_j^{\mathrm{B}} u_j^{\mathrm{X}} \end{bmatrix} \quad (16)$$

The finite difference eqs 14a−c are linearized and solved using a Gauss−Newton scheme as detailed in previous publications regarding the reactions with nonlinear kinetics.[10,11] Here we iteratively solve the equation

$$(\mathbf{M}^n - \mathbf{J}[\hat{\mathrm{N}}(\mathbf{u}^n)])\mathbf{u}^{n+1} = \mathbf{q}^n - \mathbf{J}[\hat{\mathrm{N}}(\mathbf{u}^n)]\mathbf{u}^n + \hat{\mathrm{N}}(\mathbf{u}^n) \quad (17)$$

for $\mathbf{u}^{n+1}$ until the error, e, between successive solution vectors, $\mathbf{u}^n$, drops below some given tolerance, tol. The error, e, is defined as

$$e = \sum_{i=1}^{3(N_J-1)} |u_i^n - u_i^{n+1}| \quad (18)$$

The dimensionless electrode flux is calculated from the solution vector $\mathbf{u}$ by a two-point flux approximation:[12]

$$\Psi \approx \left[\left(\frac{u_1^{\mathrm{C}} - u_0^{\mathrm{C}}}{\Delta y}\right) + \left(\frac{u_1^{\mathrm{A}} - u_0^{\mathrm{A}}}{\Delta y}\right)\right] = \left[1 + \frac{u_1^{\mathrm{C}}}{\Delta y}\right] \quad (17)$$

We also consider the effective number of electrons transferred, N_{eff}, which for the $EC_{2X}E$ reaction we define as

$$N_{\mathrm{eff}} = \frac{\Psi_{\mathrm{A}} + \Psi_{\mathrm{C}}}{\Psi_{\mathrm{A}}} = 1 + \Psi_{\mathrm{C}}$$

Computation. The simulation code was written in MATLAB 5.0 with an external call to NAG FORTRAN routines F07BDF and F07BEF to perform direct LU decomposition and solution on the banded form of matrix **M**. The nonlinear tolerance was 10^{-6}. The solution to eq 7 was achieved with the ODE45 function from the MATLAB[13] ODE toolbox. All working surface interpolation and data analysis was performed using IDL 5.0.[14]

Theoretical Results. Assuming $D_{\mathrm{A}} = D_{\mathrm{B}} = D_{\mathrm{C}} = D$, the dimensionless value N_{eff} becomes a function of only the following three variables:

$$N_{\mathrm{eff}} = N_{\mathrm{eff}}\,(k_{\mathrm{norm}}, \kappa_X, \text{and } \gamma) \quad (16)$$

Because κ_{X} is a known reaction specific parameter, it is possible to build a theoretically generated two-dimensional N_{eff} working surface as a function of the dimensionless variables k_{norm} and γ. We therefore consider the form of the working surface for the test case where $\kappa_{\mathrm{X}} = 1$ with reference to the $EC_{2X}E$ reaction at a microdisk electrode. Simulations were accordingly run with 25 points in the ranges $-4 \le k_{\mathrm{norm}} \le 8$ and $0 \le \gamma \le 1.0$ with $N_J = 200$, which according to previous literature, is sufficient for an accuracy considerably less than experimental error.[15] A diagram of the resulting working surface is shown in Figure 1.

Later we illustrate how working surface interpolation (WSI) of simulation generated data may be used as a method for a quantitative determination of the rate constant k_2 in the $EC_{2X}E$ reaction.[6]

Experimental Section

All reagents were obtained from Aldrich and were of the highest grade available and used without further purification.

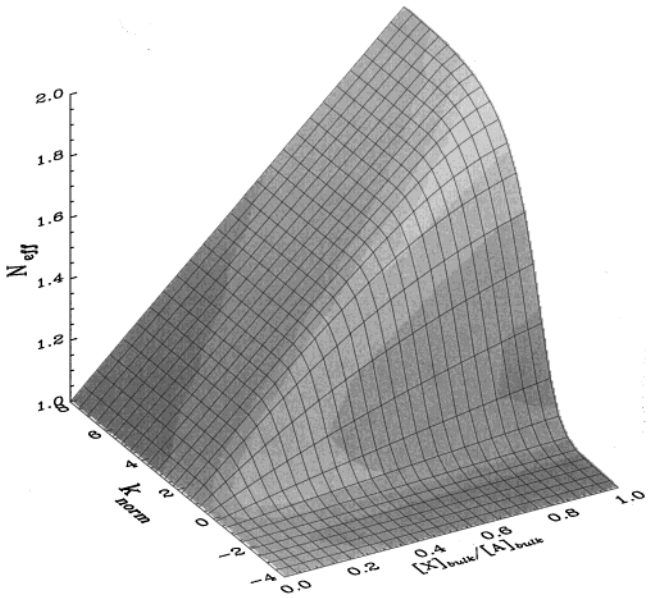

Figure 1. Diagram of the working surface of N_{eff} for the $EC_{2X}E$ reaction at a rotating disk electrode ($\gamma = 1.0$; $\kappa_X = 1.00$).

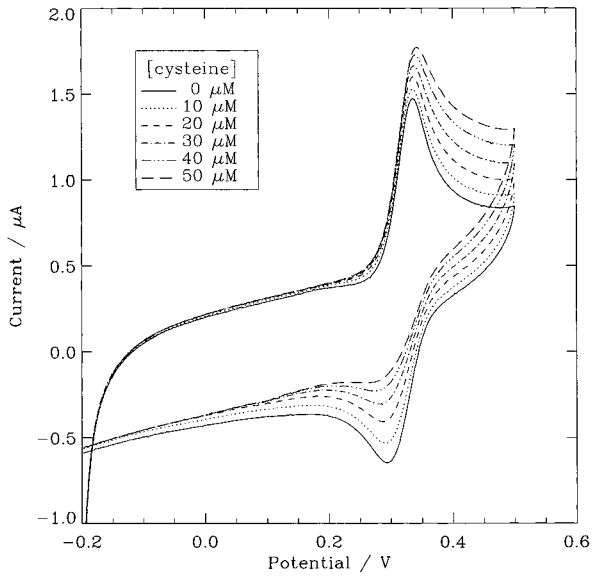

Figure 2. Cyclic voltammogram (scan rate of 2 mV s^{-1}) of the paracetamol (50 μM) in hydrostatic conditions with sequential additions of cysteine (10 μM).

All solutions and subsequent dilutions were prepared using deionized water from an Elgastat (Elga, UK) UHQ grade water system with a resistivity of 18 MΩ cm. All solutions were degassed and stored under argon and used within 12 h to minimize degradation.

All electrochemical measurements were recorded using a μ Autolab computer-controlled potentiostat (Eco-Chemie, Netherlands) with a standard three-electrode configuration. A 3 mm glassy carbon electrode (BAS) served as the working electrode, platinum wire wound into a spiral provided the counter electrode, with a saturated calomel reference electrode (SCE, Radiometer, Copenhagen) completing the cell assembly.

Rotating disk analysis was conducted using an Oxford electrode motor controller. The glassy carbon electrode was sheathed in Teflon with a brass thread, allowing connection to the motor, and was rotated at differing speeds (2−25 Hz).

SCHEME 1

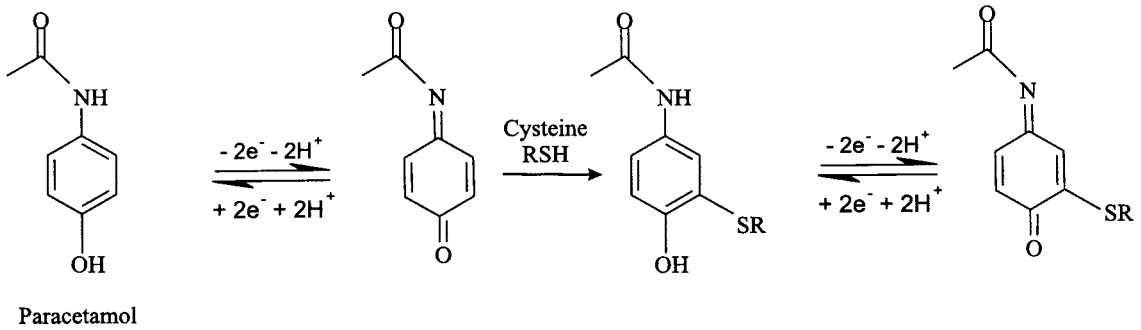

Paracetamol

Results and Discussion

Hydrostatic cyclic voltammetry at a scan rate of 20 mV s^{-1} was used to observe the voltammetric features of both pure 4-acetamidophenol (50 μM, pH 7, 0.1 M Na_2HPO_4/NaH_2PO_4, 0.1 M KCl) and paracetamol in the presence of added cysteine (10 μM). As can be seen in Figure 2, in the absence of cysteine, the voltammogram shows an oxidative peak at +0.34 V and a corresponding reduction peak at +0.29 V, consistent with an electrochemically reversible process. Also, the sequential addition of aliquots of cysteine produces an enhancement in the paracetamol oxidation peak current and a corresponding decrease in the reduction peak current. Both effects are consistent with analogous sulfydryl thiol−phenylene[1−5,16] electrochemistry. For the paracetamol/cysteine system, the electrochemically initiated reaction process can be ascribed primarily to the electrochemical oxidation of paracetamol to a quinone intermediate. This intermediate then reacts with cysteine to form a cysteine−paracetamol adduct, which is immediately oxidized at the electrode surface (Scheme 1), giving the enhancement in peak current. The corresponding decrease in the reduction peak is due to a depletion in the amount of oxidized paracetamol.

Preliminary modeling of the reaction step between the intermediate quinone and cysteine was conducted using DIGISIM (BAS Technicol)[17] to generate the cyclic voltammetry data, such as that shown in Figure 2. The diffusion coefficients of the cysteine and paracetamol were estimated using the Wilke−Chang[18] relationship:

$$D = 7.4 \times 10^{-8} \frac{(\chi M)^{1/2} T}{\nu V^{0.6}}$$

where T is the temperature of the solution in kelvin, M is the molecular weight of the solvent, χ is the association parameter (equal to 2.6 in this case), ν is the viscosity (0.89 cP in the case of water at 25 °C), and V is the molar volume of the solute at the normal boiling point estimated for complex molecules from atomic contributions as defined by La Bas.[19] The diffusion coefficients obtained were paracetamol (7.88×10^{-6} cm^2 s^{-1}) and cysteine (2.46×10^{-5} cm^2 s^{-1}). DIGISIM results for a planar electrode, as illustrated in Figure 3, showed that best agreement with the observed experimental peak current data was obtained at a value of $k_2 = 1.25 \pm 0.25 \times 10^7$ mol^{-1} cm^3 s^{-1}.

Rotating disk steady-state linear sweep voltammetry experiments were next performed in order to validate the numerical modeling for the paracetamol system transport limited steady-state problem. These were carried out by measuring the limiting currents at differing concentrations of cysteine (20−120 μM) and a fixed concentration of paracetamol (100 μM, pH 7, 23 ± 2 °C). The voltammograms were recorded between +0.1 and +0.7 V (2 mV s^{-1}) and at five rotational speeds of 2, 4, 8, 16, and 25 Hz. In all cases, a single reversible two-electron wave was observed with $E_{1/2} = +0.37$ V vs SCE, and the addition of cysteine produced an enhancement of the kinetically activated steady-state current. Analysis of the linear sweep voltammograms provided a method to determine quantitatively the transport limited steady-state current, which was used in all of the subsequent modeling.

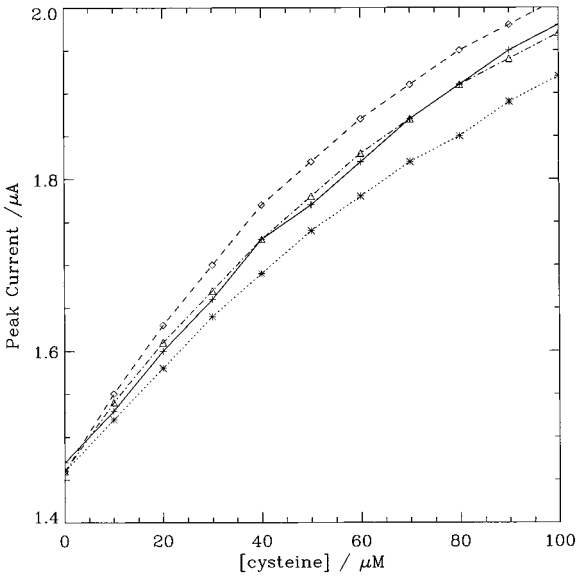

Figure 3. Plots of variation of experimental (+) and theoretical ($k_2 = 1.0 \times 10^7$(*), 1.25×10^7 (△), 1.5×10^7 (◇) cyclic voltammetry peak currents in hydrostatic conditions with change in cysteine concentration at constant paracetamol concentration (100 μM).

We begin the analysis of the experimental data by seeking an optimized value of κ_X, which will enable the generation of a simulation based working surface. Using the Levich equation[20] for laminar conditions in conjunction with the transport limited currents for the five different rotation speeds in the absence of cysteine, a mean value of $D_A = 6.7 \times 10^{-6}$ cm s^{-1} was obtained, which is consistent with similar small systems such as hydroquinone, aminophenol, etc.[20,21] The Wilke−Chang calculated value of $D_{cysteine}(D_X) = 2.48 \times 10^{-5}$ cm s^{-1} was used in all modeling. Simulations were accordingly run for this value of $\kappa_X = 3.70$ with 25 points in the ranges $-2 \le k_{norm} \le 4$ and $0 \le \gamma \le 1.2$ with $N_J = 200$, which, according to previous literature, is sufficient for an accuracy within experimental error.[22] By interpolating experimentally controlled γ values onto the working surface and comparing the interpolated and experimental values of N_{eff}, we aim to find an optimum value of k_{norm} (k_{norm}^{opt}) for each of the five data series collected for the five different rotational speeds. Previous research shows that for working surfaces of sizes close to 25×25 points, the bilinear

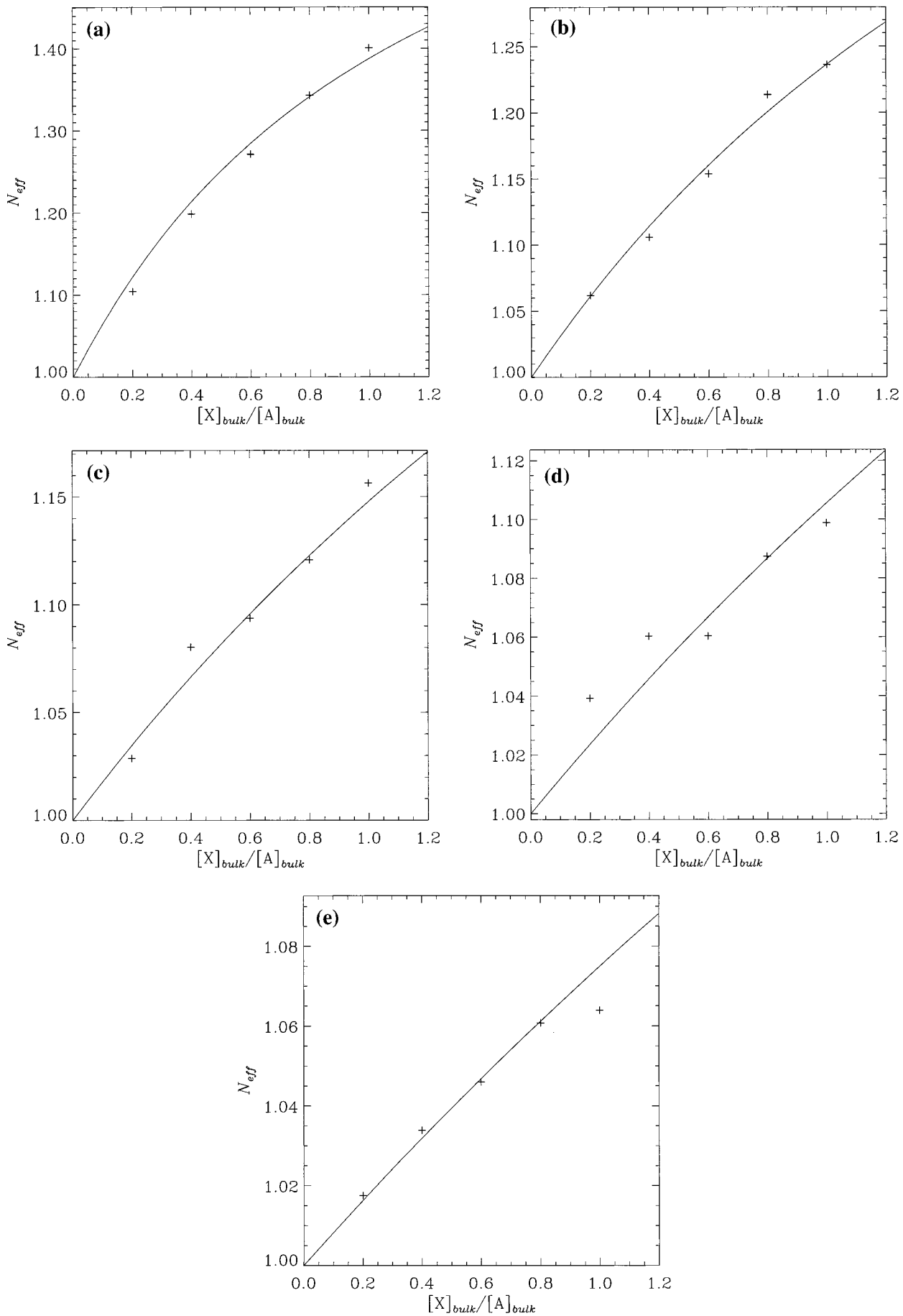

Figure 4. Plots showing experimental N_{eff} data (+) for the paracetamol/cysteine system and theoretically calculated N_{eff} data (−) at $k_{\text{norm}}^{\text{opt}}$ for the $EC_{2X}E$ reaction at a scan rate of (a) 2, (b) 4, (c) 8, (d) 16, and (e) 25 Hz.

TABLE 1: Kinetic Results Derived from Experimental Data

W/Hz	$\log(k_{norm}^{opt})$	k_{norm}^{opt}	k_2/mol^{-1} cm^3 s^{-1}	ϵ/%	$\bar{e}_{current}$/%
2	0.342	1.408	1.5×10^7	0.0	1.6
4	−0.024	0.976	1.3×10^7	0.0	2.3
8	−0.306	0.736	1.4×10^7	0.0	13.7
16	−0.480	0.618	1.9×10^7	−0.2	4.0
25	−0.661	0.517	1.9×10^7	0.0	3.5

interpolation option of the INTERPOLATE function in IDL 5.0 provides satisfactory results with minimal programming,[11] and hence this method was chosen.

When using the WSI for the determination of the rate constant in the $EC_{2X}E$ reaction, it is assumed that the value of N_{eff} is unity in the absence of redox mediation, i.e., when the concentration of sulfide is zero. In this investigation we also assume that any significant error, ϵ, in the experimental limiting currents in the absence of the redox mediation will systematically propagate through the experimental N_{eff} data set. Hence, to find the value of k_{norm}^{opt}, we need to minimize the interpolation errors in not only k_{norm} but also ϵ. For this work, we define exactly the interpolation error as 1 − norm of the difference between surface and interpolated data at any values of ϵ and k_{norm}. WSI was therefore carried out on the five experimental data sets, with the criteria described above. Figures 4a−e illustrate the quality of fit between the experimentally determined N_{eff} data and that generated from k_{norm}^{opt}. The tabulated results for rate constants k_{norm}^{opt}, k_2, ϵ, and the resulting mean relative standard deviation between predicted and experimental current ($\bar{e}_{current}$) are given in Table 1. The average optimized value of k_2 over the five experiments is 1.6×10^7 mol^{-1} cm^3 s^{-1} and has a percentage relative standard deviation of 22%. This compares well with the DIGISIM derived result of $k_2 = 1.25 \pm 0.25 \times 10^7$ mol^{-1} cm^3 s^{-1}.

Conclusions

A general method for modeling the transport-limited current for the $EC_{2X}E$ reaction at the rotating disk electrode has been illustrated. It has been shown that this method allows easy working surface interpolation of experimental data so that a rate constant for the redox-mediated step in the $EX_{2X}E$ reaction may be investigated. The results of this method are shown to be in good agreement, with the value of the rate constant derived form hydrostatic cyclic voltammetric data and modeling using the commercial package DIGISIM.

Acknowledgment. We thank EPSRC, Windsor Scientific, and Schlumberger for CASE studentships for B.A.B. and N.S.L.

References and Notes

(1) Lawrence, N. S.; Davis, J.; Compton, R. G. *Talanta* **2000**, *52*, 771.
(2) Lawrence, N. S.; Davis, J.; Compton, R. G. *Talanta* **2000**, *53*, 1089.
(3) Lawrence, N. S.; Davis, J.; Jiang, L.; Jones, T. G. J.; Davies, S. N.; Compton, R. G. *Electroanalysis* **2000**, *12*, 1453.
(4) Lawrence, N. S.; Davis, J.; Marken, F.; Jiang, L.; Jones, T. G. J.; Davies, S. N.; Compton, R. G. *Electroanalysis* **2000**, *69*, 189.
(5) Lawrence, N. S.; Davis, J.; Jiang, L.; Jones, T. G. J.; Davies, S. N.; Compton, R. G. *Analyst* **2000**, *125*, 661.
(6) Brookes, B. A.; Lawrence, N. S.; Compton, R. G. C. *J. Phys. Chem B* **2000**, *104*, 11258.
(7) Albery, W. J. *Electrode kinetics*; Clarendon Press:Oxford, 1975.
(8) Hale, J. M. *J. Electroanal. Chem.* **1963**, *6*, 187.
(9) Hale, J. M. *J. Electroanal. Chem.* **1964**, *8*, 332.
(10) Alden, J. A.; Compton, R. G. *J. Phys. Chem. B* **1997**, *101*, 8941.
(11) Alden, J. A.; Compton, R. G. *J. Phys. Chem. B* **1997**, *101*, 9741.
(12) A flux approximation involving more than two points will lead to inaccuracies at high rate constants due to the singularity that develops in the concentration distribution of the C species adjacent to the electrode surface (see ref 6). This singularity may be overcome with finer meshing; however, this significantly increases computational demands.
(13) http://www.mathworks.co.uk.
(14) http://www.floating.co.uk/idl.
(15) Increasing N_J from 200 to 1000 resulted in a maximum discrepancy of 4.4×10^{-3} in the value of N_{eff} with $\gamma = 1.0$; $\kappa_X = 1.0$.
(16) White, P. C.; Lawrence, N. S.; Davis. J.; Compton, R. G. *Anal. Chim. Acta*, submitted 2001.
(17) Rudolph, M.; Reddy, D. P.; Feldberg, S. W. *Anal. Chem.* **1994**, *66*, 589.
(18) Wilke, C. R.; Chang, P. *AIChE J* **1955**, *1*, 264.
(19) Perry, J. H. *Chemical Engineers Handbook*; McGraw-Hill: New York, 1950.
(20) Bard, A. J.; Faulkner, L. R. *Electrochemical Methods*, 2nd ed.; Wiley: New York, 2001.
(21) Adams, R. N. *Electrochemistry at solid surface electrodes*; Marcel Dekker: New York, 1969; p 356.
(22) Increasing N_J from 100 to 1000 resulted in a maximum discrepancy of 0.0044 in the value of N_{eff}.